

EPTT-2022-0009

STABILITY ANALYSIS OF VISCOELASTIC FLUID FLOWS IN BOUNDARY LAYER

Beatriz Liara Carreira

Leandro Franco de Souza

Universidade de São Paulo, Instituto de Ciências Matemáticas e de Computação, São Carlos
liara.carreira@usp.br, lefraso@icmc.usp.br

Analice Costacurta Brandi

Universidade Estadual Paulista “Júlio de Mesquita Filho”, Faculdade de Ciências e Tecnologia, Presidente Prudente
analice.brandi@unesp.br

Abstract. *A laminar flow is always subject to small disturbances that can occur due to several factors, such as structural vibration, surface roughness, noise, external turbulence, etc. If these disturbances are not dampened, the laminar flow evolves into a more complex state but not necessarily a turbulent state. This process, known as the laminar-turbulent transition, is extremely complex and not completely understood, especially for non-Newtonian fluid flows. A complete understanding of the transition process, with consequent ability to control, would open up great perspectives in science and industry. Hydrodynamic stability analysis is carried out with this objective. In the boundary layer, the transition can occur due to the convection of Tollmien-Schlichting waves. Thus, the objective of this work is to investigate the hydrodynamic stability in a two-dimensional, incompressible and isothermal flow of a Giesekus viscoelastic fluid over a flat plate through the analysis of Tollmien-Schlichting wave convection using the Linear Stability Theory.*

Keywords: *Giesekus fluid, linear stability theory, boundary layer, laminar-turbulent transition*

1. INTRODUCTION

Knowledge of the flow regime, be it laminar, transitional or turbulent, is necessary for the correct design of aerodynamic surfaces or cooling systems (Souza *et al.*, 2005). In many scientific and industrial applications, the stability of laminar flow and the transition to turbulence are relevant (Brandi *et al.*, 2019). Therefore, it is essential to investigate the physics of stability and the laminar-turbulent transition to control, advance or prevent it (Gervazoni, 2016).

Due to the great need of the industry to simulate viscoelastic fluid flows and the great complexity of treating this type of problem, an enormous amount of resources have been invested in the development of new technologies and numerical methods capable of predicting, at low costs and with good results, the behaviour of these flows. One of the focuses of interest is to predict complex phenomena that can result from viscoelastic behaviour, for example.

For any flow, the transition to turbulence can be generalized as the result of the amplification of disturbances injected into the flows by different sources. The physical form of the generation of instabilities from a disturbance will depend on the flow type. It may be related to several factors, such as structural vibration, surface roughness, noise, and external turbulence, among others. If these disturbances are not dampened, the laminar flow undergoes a transition to another more complex state, but not necessarily a turbulent flow state (Souza *et al.*, 2005). The relationship between the disturbance and the transition process to the turbulent regime of a flow is part of the investigation of the hydrodynamic stability (Zhang *et al.*, 2013).

In particular, non-Newtonian laminar boundary layer flows are observed in several domains, including biological and chemical systems, food processing engineering systems or pharmaceutical processing (Amoo and Fagbenle, 2020). Since most of the differences between categories of non-Newtonian fluids are related to their viscosity, a dominant physical property within the boundary layer region, a thorough understanding of these flows is of considerable importance for various industrial applications (Amoo and Fagbenle, 2020).

A paradox was encountered when stability theory researchers realized that a laminar boundary layer transitioned to turbulence, even though its stability was theoretically guaranteed due to the inexistence of inflexion points. The researchers noticed the propagation of waves in the boundary layer, which became known as Tollmien-Schlichting waves.

Therefore, this work uses the Linear Stability Theory to investigate the convection of Tollmien-Schlichting waves in a boundary layer flow over a flat plate, considering a viscoelastic fluid from the Giesekus model. Different cases were tested by varying the dimensionless parameters that characterize non-Newtonian fluids to analyze how elastic forces and the polymeric contribution of the fluid can influence the spatial stability of viscoelastic flow and compare them with Newtonian fluid flows.

2. MATHEMATICAL FORMULATION

The flow is assumed to be unsteady, non-Newtonian, two-dimensional and incompressible. The conservation of mass (continuity) and conservation of momentum equations governing the flow, in the dimensionless form, are given by

$$\nabla \cdot \mathbf{u} = 0, \quad (1)$$

$$\frac{\partial \mathbf{u}}{\partial t} + \nabla \cdot (\mathbf{u}\mathbf{u}) = -\nabla p + \frac{\beta}{Re} \nabla^2 \mathbf{u} + \nabla \cdot \mathbf{T}, \quad (2)$$

where \mathbf{u} denotes the velocity field, t is the time, p is the pressure and \mathbf{T} is the non-Newtonian extra-stress tensor (symmetric), given by $\mathbf{T} = \begin{bmatrix} T^{xx} & T^{xy} \\ T^{xy} & T^{yy} \end{bmatrix}$.

The dimensionless parameter $Re = U_\infty L / \nu$ is associated with the Reynolds number, where L and U_∞ denote length and velocity scales, respectively, and ν is the kinematic viscosity of the fluid. The amount of Newtonian solvent is controlled by the dimensionless solvent viscosity coefficient $\beta = \eta_s / \eta_0$, where $\eta_0 = \eta_s + \eta_p$ denotes the total shear viscosity, being η_s and η_p the Newtonian solvent and polymeric viscosities, respectively.

In this paper, we worked with viscoelastic fluid flow governed by the non-linear Giesekus constitutive equation (Giesekus, 1982), which is given by

$$\mathbf{T} + Wi \overset{\nabla}{\mathbf{T}} + \alpha_G \frac{Wi Re}{1 - \beta} (\mathbf{T} \cdot \mathbf{T}) = \frac{1 - \beta}{Re} (\nabla \mathbf{u} + \nabla \mathbf{u}^\top), \quad (3)$$

where α_G is the mobility parameter that regulates the shear thinning behavior of the fluid ($0 \leq \alpha_G \leq 1$), $\mathbf{T} \cdot \mathbf{T}$ is a tensor product and $\overset{\nabla}{\mathbf{T}}$ is the upper-convected derivative. The dimensionless parameter $Wi = \lambda U_\infty / L$ is called Weissenberg number, being λ the relaxation-time of the fluid.

3. LINEAR STABILITY THEORY

Linear Stability Theory assumes that instantaneous flow can be decomposed into a base and disturbed flow. In particular, in this work, we consider the non-parallel base flow,

$$\mathbf{u}(x, y, t) = \mathbf{U}(x, y) + \tilde{\mathbf{u}}(x, y, t), \quad p(x, y, t) = P(x, y) + \tilde{p}(x, y, t), \quad \mathbf{T}(x, y, t) = \hat{\mathbf{T}}(x, y) + \tilde{\mathbf{T}}(x, y, t),$$

where for a two-dimensional flow, $\mathbf{u} = (u, v)$, $\mathbf{U} = (U, V)$, $\tilde{\mathbf{u}} = (\tilde{u}, \tilde{v})$, $\mathbf{T} = (T^{xx}, T^{xy}, T^{yy})$, $\hat{\mathbf{T}} = (\hat{T}^{xx}, \hat{T}^{xy}, \hat{T}^{yy})$ and $\tilde{\mathbf{T}} = (\tilde{T}^{xx}, \tilde{T}^{xy}, \tilde{T}^{yy})$, and the disturbances can be written generally as

$$\tilde{\mathbf{u}} = \bar{\mathbf{u}}(y) e^{i(\alpha x - \omega t)}, \quad \tilde{p} = \bar{p}(y) e^{i(\alpha x - \omega t)}, \quad \tilde{\mathbf{T}} = \bar{\mathbf{T}}(y) e^{i(\alpha x - \omega t)},$$

where $i = \sqrt{-1}$, $\bar{\mathbf{u}} = (\bar{u}, \bar{v})$ and $\bar{\mathbf{T}} = (\bar{T}^{xx}, \bar{T}^{xy}, \bar{T}^{yy})$. These equations indicate that disturbances propagate as waves with frequency ω , wave-length $\lambda = 2\pi/\alpha$, wave velocity $c = \omega/\alpha$, where α is the wave number in the x direction, and amplitudes $\bar{\mathbf{u}}$, \bar{p} and $\bar{\mathbf{T}}$. Thus, using the separating variables method by normal modes, the system composed of conservation equations and non-Newtonian tensor equations is reduced to a system of differential equations (Furlan, 2018),

$$i\alpha \bar{u} + \frac{d\bar{v}}{dy} = 0, \quad (4)$$

$$\left(-i\omega + \frac{\partial U}{\partial x}\right) \bar{u} + V \frac{d\bar{u}}{dy} - \frac{\beta}{Re} \frac{d^2 \bar{u}}{dy^2} + \frac{\partial U}{\partial y} \bar{v} - \frac{d\bar{T}^{xy}}{dy} = \left(-\alpha i U - \frac{\beta}{Re} \alpha^2\right) \bar{u} - \alpha i \bar{p} + \alpha i \bar{T}^{xx}, \quad (5)$$

$$\frac{\partial V}{\partial x} \bar{u} + \left(-i\omega + \frac{\partial V}{\partial y}\right) \bar{v} + V \frac{d\bar{v}}{dy} - \frac{\beta}{Re} \frac{d^2 \bar{v}}{dy^2} + \frac{d\bar{p}}{dy} - \frac{d\bar{T}^{yy}}{dy} = \left(-\alpha i U - \frac{\beta}{Re} \alpha^2\right) \bar{v} + \alpha i \bar{T}^{xy}, \quad (6)$$

$$\begin{aligned} Wi \frac{\partial \hat{T}^{xx}}{\partial x} \bar{u} - 2Wi \hat{T}^{xy} \frac{d\bar{u}}{dy} + Wi \frac{\partial \hat{T}^{xx}}{\partial y} \bar{v} + \left(1 + Wi \left(-i\omega + 2\frac{\partial U}{\partial x}\right) + \alpha_G \frac{Wi Re}{1 - \beta} 2\hat{T}^{xx}\right) \bar{T}^{xx} + Wi V \frac{d\bar{T}^{xx}}{dy} + \\ + \left(-2Wi \frac{\partial U}{\partial y} + \alpha_G \frac{Wi Re}{1 - \beta} 2\hat{T}^{xy}\right) \bar{T}^{xy} = \left(2Wi \alpha i \hat{T}^{xx} + 2\frac{1 - \beta}{Re} i \alpha\right) \bar{u} - Wi U i \alpha \bar{T}^{xx}, \end{aligned} \quad (7)$$

$$\begin{aligned}
& Wi \frac{\partial \hat{T}^{xy}}{x} \bar{u} - \left(Wi \hat{T}^{yy} + \frac{1-\beta}{Re} \right) \frac{d\bar{u}}{dy} + Wi \frac{\partial \hat{T}^{xy}}{\partial y} \bar{v} + \left(-Wi \frac{\partial V}{\partial x} + \alpha_G \frac{Wi Re}{1-\beta} \hat{T}^{xy} \right) \bar{T}^{xx} + \\
& + \left(1 - Wi \omega_i + \alpha_G \frac{Wi Re}{1-\beta} (\hat{T}^{xx} + \hat{T}^{yy}) \right) \bar{T}^{xy} + Wi V \frac{d\bar{T}^{xy}}{dy} + \left(-Wi \frac{\partial U}{\partial y} + \alpha_G \frac{Wi Re}{1-\beta} \hat{T}^{xy} \right) \bar{T}^{yy} = \\
& = \left(Wi \alpha_i \hat{T}^{xx} + \frac{1-\beta}{Re} i \alpha \right) \bar{v} - Wi U i \alpha \bar{T}^{xy}, \tag{8}
\end{aligned}$$

$$\begin{aligned}
& Wi \frac{\partial \hat{T}^{yy}}{x} \bar{u} - 2 \left(Wi \hat{T}^{yy} + \frac{1-\beta}{Re} \right) \frac{d\bar{v}}{dy} + Wi \frac{\partial \hat{T}^{yy}}{\partial y} \bar{v} + \left(-2Wi \frac{\partial V}{\partial x} + \alpha_G \frac{Wi Re}{1-\beta} 2\hat{T}^{xy} \right) \bar{T}^{xy} + \\
& + \left(1 + Wi \left(-i\omega - 2 \frac{\partial V}{\partial y} \right) + \alpha_G \frac{Wi Re}{1-\beta} 2\hat{T}^{yy} \right) \bar{T}^{yy} = \left(2Wi \alpha_i \hat{T}^{xy} \right) \bar{v} - Wi U i \alpha \bar{T}^{yy}. \tag{9}
\end{aligned}$$

3.1 Numerical Method

In particular, for two-dimensional perturbations, if ω ($\omega_i = 0$ and $\omega = \omega_r$) is a real number and α is a complex number, then the perturbation amplitude is increasing in the direction of the mean flow x . The components ω_r , α_r and α_i represent, respectively, the frequency, the wave number and the spatial amplification rate, in which case the formulation is called a spatial formulation.

Now, if α is a real number and ω is a complex number, we have the perturbation amplitude increasing as a time function. In this case, the formulation is called the temporal formulation, and ω_i is the temporal amplification rate. The classification of instabilities, depending on the temporal and spatial analyses, is presented in Tab. 1.

Table 1. Instabilities classification.

Type of analysis	Amplification rate	Amplitude	Classification
Spatial analysis	$\alpha_i < 0$	increase	unstable
	$\alpha_i = 0$	constant	neutral
	$\alpha_i > 0$	decreases	stable
Temporal analysis	$\omega_i < 0$	decreases	stable
	$\omega_i = 0$	constant	neutral
	$\omega_i > 0$	increase	unstable

In this work, the spatial analysis is performed considering the system composed by the conservation Eqs. (4) – (9), from which it is possible to write the following system

$$\mathbf{M} [\bar{u} \quad \alpha \bar{u} \quad \bar{v} \quad \alpha \bar{v} \quad \bar{p} \quad \bar{T}^{xx} \quad \bar{T}^{xy} \quad \bar{T}^{yy}]^\top = \alpha \mathbf{Q} [\bar{u} \quad \alpha \bar{u} \quad \bar{v} \quad \alpha \bar{v} \quad \bar{p} \quad \bar{T}^{xx} \quad \bar{T}^{xy} \quad \bar{T}^{yy}]^\top, \tag{10}$$

where \mathbf{M} and \mathbf{Q} are matrices constructed in such a way that the Eq. (10) is equivalent to the system composed by Eqs. (4) – (9). Thus, the instability modes are obtained by solving an eigenvalue problem, for which the first and second ordinary derivatives with respect to y are calculated using differentiation matrices based on the Chebyshev polynomial (Don and Solomonoff, 1995).

3.2 Base Flow

We consider the Blasius solution (Schlichting, 1979) to calculate the base flow. A direct numerical simulation is performed using the velocity and vorticity components from the Blasius solution as initial conditions to eliminate possible inconsistencies and obtain the values U , V , \hat{T}^{xx} , \hat{T}^{xy} and \hat{T}^{yy} .

In the direct numerical simulation, to simplify the problem and eliminate the pressure treatment in the momentum equations, we chose the vorticity-velocity formulation (Brandi *et al.*, 2017). Then, the two-dimensional vorticity ω_z is defined by

$$\omega_z = \frac{\partial u}{\partial y} - \frac{\partial v}{\partial x}. \tag{11}$$

Applying such formulation, therefore, the direct numerical simulation code resolves the system composed by Eqs. (12) – (17),

$$\frac{\partial U}{\partial x} + \frac{\partial V}{\partial y} = 0, \quad (12)$$

$$\frac{\partial^2 V}{\partial x^2} + \frac{\partial^2 V}{\partial y^2} = -\frac{\partial \hat{\omega}_z}{\partial x}, \quad (13)$$

$$\frac{\partial \hat{\omega}_z}{\partial t} + \frac{\partial \hat{\omega}_z}{\partial x} U + \frac{\partial \hat{\omega}_z}{\partial y} V = \frac{\beta}{Re} \left[\frac{\partial^2 \hat{\omega}_z}{\partial x^2} + \frac{\partial^2 \hat{\omega}_z}{\partial y^2} \right] - \frac{\partial^2 \hat{T}^{xy}}{\partial x^2} - \frac{\partial^2 \hat{T}^{yy}}{\partial x \partial y} + \frac{\partial^2 \hat{T}^{xx}}{\partial y \partial x} + \frac{\partial^2 \hat{T}^{xy}}{\partial y^2}, \quad (14)$$

$$\begin{aligned} \hat{T}^{xx} + Wi \left(\frac{\partial \hat{T}^{xx}}{\partial t} + U \frac{\partial \hat{T}^{xx}}{\partial x} + V \frac{\partial \hat{T}^{xx}}{\partial y} - 2\hat{T}^{xx} \frac{\partial U}{\partial x} - 2\hat{T}^{xy} \frac{\partial U}{\partial y} \right) + \alpha_G \frac{WiRe}{1-\beta} \left(\hat{T}^{xx^2} + \hat{T}^{xy^2} \right) = \\ = 2 \frac{1-\beta}{Re} \frac{\partial U}{\partial x}, \end{aligned} \quad (15)$$

$$\begin{aligned} \hat{T}^{xy} + Wi \left(\frac{\partial \hat{T}^{xy}}{\partial t} + U \frac{\partial \hat{T}^{xy}}{\partial x} + V \frac{\partial \hat{T}^{xy}}{\partial y} - \hat{T}^{xx} \frac{\partial V}{\partial x} - \hat{T}^{yy} \frac{\partial U}{\partial y} \right) + \alpha_G \frac{WiRe}{1-\beta} \left(\hat{T}^{xy} \left(\hat{T}^{xx} + \hat{T}^{yy} \right) \right) = \\ = \frac{1-\beta}{Re} \left(\frac{\partial V}{\partial x} + \frac{\partial U}{\partial y} \right), \end{aligned} \quad (16)$$

$$\begin{aligned} \hat{T}^{yy} + Wi \left(\frac{\partial \hat{T}^{yy}}{\partial t} + U \frac{\partial \hat{T}^{yy}}{\partial x} + V \frac{\partial \hat{T}^{yy}}{\partial y} - 2\hat{T}^{xy} \frac{\partial V}{\partial x} - 2\hat{T}^{yy} \frac{\partial V}{\partial y} \right) + \alpha_G \frac{WiRe}{1-\beta} \left(\hat{T}^{xy^2} + \hat{T}^{yy^2} \right) = \\ = 2 \frac{1-\beta}{Re} \frac{\partial V}{\partial y}, \end{aligned} \quad (17)$$

where Eq. (12) is the continuity equation, Eq. (13) is the Poisson equation for the V velocity component, obtained deriving Eq. (11) with respect to x . Equation (14) is obtained by deriving the momentum equation in direction y with respect to x and subtracting the derivative of the momentum equation in direction x with respect to y . Finally, Eqs. (15) – (17) are the Giesekus model equations for the non-Newtonian tensor in two-dimensional cartesian coordinates.

4. NUMERICAL RESULTS

The following results were obtained through the Linear Stability Theory from a base flow generated in a Direct Numerical Simulation from the Blasius solution. In order to investigate the hydrodynamic stability of the flow, the simulation considered $U_\infty = 15.90m/s$, $L = 0.1m$ and $\nu = 1.59 \times 10^{-5}m^2/s$, resulting in a Reynolds number $Re = 100000$.

For base flow, the domain of numerical integration extends from $x_0 = 1.0$ to $x_{max} = 4.22$ in the streamwise direction and from $y_0 = 0$ to $y_{max} = 0.77 \times 10^{-1}$ in the normal direction. The following parameters were adopted for the numerical simulation: the number of points in the streamwise and normal directions are $imax = 537$ and $jmax = 129$, respectively, being the distance between two consecutive points in the direction x , $\Delta x = 0.006$. Discretization in the y direction was performed using a mesh with a stretch factor of 10%.

Figures 1 and 2 represent the boundary layer profile obtained in non-Newtonian fluid flow for variations of $\beta = 0.90, 0.70$ and 0.50 , with $\alpha_G = 0.30$ fixed and $Wi = 1$ and 10 . To verify the effect of the non-Newtonian contribution, the non-Newtonian profile is shown in comparison with the same profile in the Newtonian fluid flow. Therefore, in Figs. 1(a) and 2(a), the boundary layer velocity profile U at the streamwise position $x = 3.148$ was shown as a function of the dimensionless coordinate

$$\eta = y \sqrt{\frac{U_\infty}{\nu x}}.$$

In addition, Figs. 1(b) and 2(b) contain the relative variation between the non-Newtonian solution and the Newtonian solution. The variation calculation was performed as follows

$$E_U = \frac{U_{nNewt} - U_{Newt}}{U_{Newt}},$$

where U_{Newt} and U_{nNewt} represent Newtonian and non-Newtonian solutions, respectively. It can be noted that the velocity in the boundary layer is higher in the non-Newtonian case and increases as β decreases. Also, the greatest variation appears near the wall.

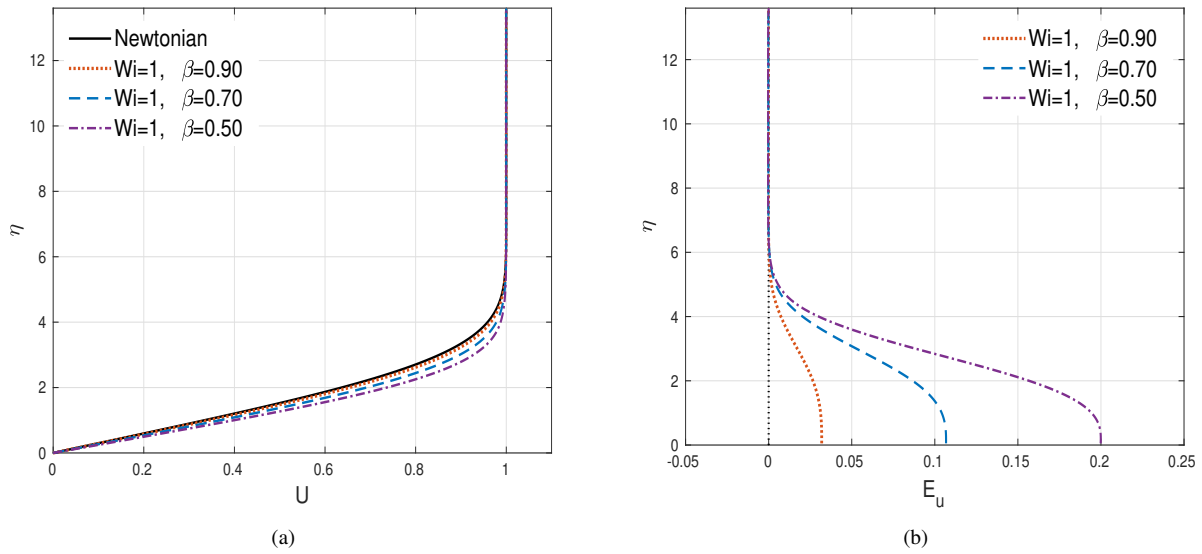


Figure 1. Comparison between velocity profiles in the boundary layer for $Wi = 1$.

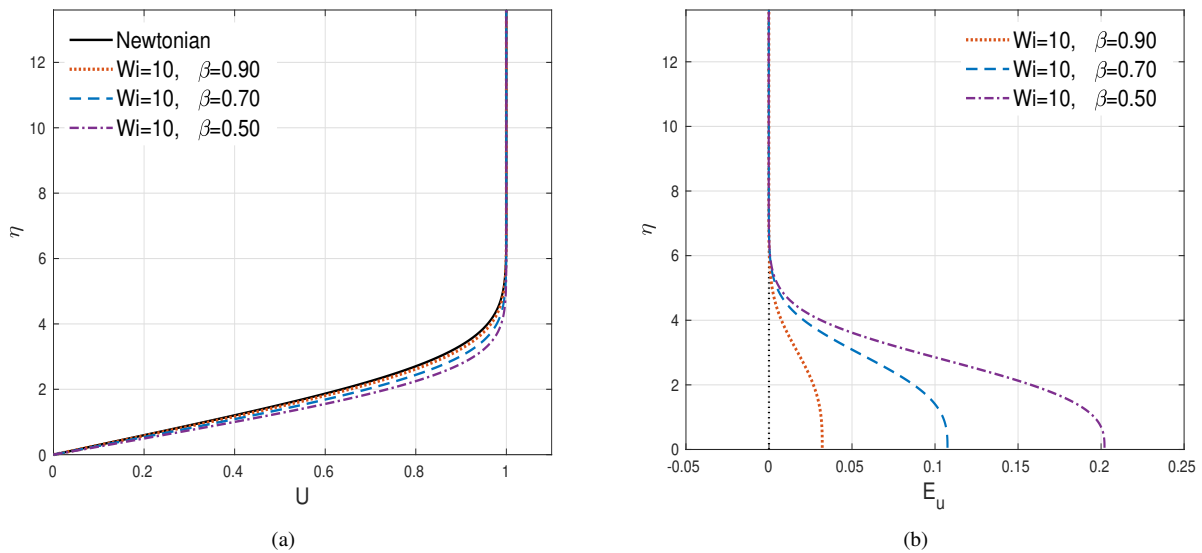


Figure 2. Comparison between velocity profiles in the boundary layer for $Wi = 10$.

Comparing the results obtained for Newtonian and non-Newtonian flows, a variation of the constants that characterize the viscoelastic fluid is performed to verify these dimensionless parameters influence on the flow's stability. The parameter α_G was fixed at 0.30 and so we changed $\beta = 0.50, 0.70$ and 0.90 to $Wi = 1, 5, 10$ and 25 . Numerical simulations provided the values of the spatial amplification rates α_i for each case. As a spatial analysis, amplification rates less than zero ($\alpha_i < 0$) characterize flow instability and amplification rates greater than zero ($\alpha_i > 0$) characterize stability.

In that sense, Fig. 3 presents the spatial growth rate ($-\alpha_i$) as a function of the frequency ω , where it can be easily verified that non-Newtonian flows reach a higher amplification rate in relation to Newtonian flow, and this is more evident as the value of β decreases, that is when there is a more significant non-Newtonian contribution in the fluid. The same happens when the value of the Weissenberg number, Wi , is increased.

Another important observation is that there is a more significant influence with the variation of Wi in fluids with a more significant polymeric contribution. Furthermore, for these cases, when β decreases, the range of unstable frequencies increases as the frequency at which the flow returns to stabilize increases.

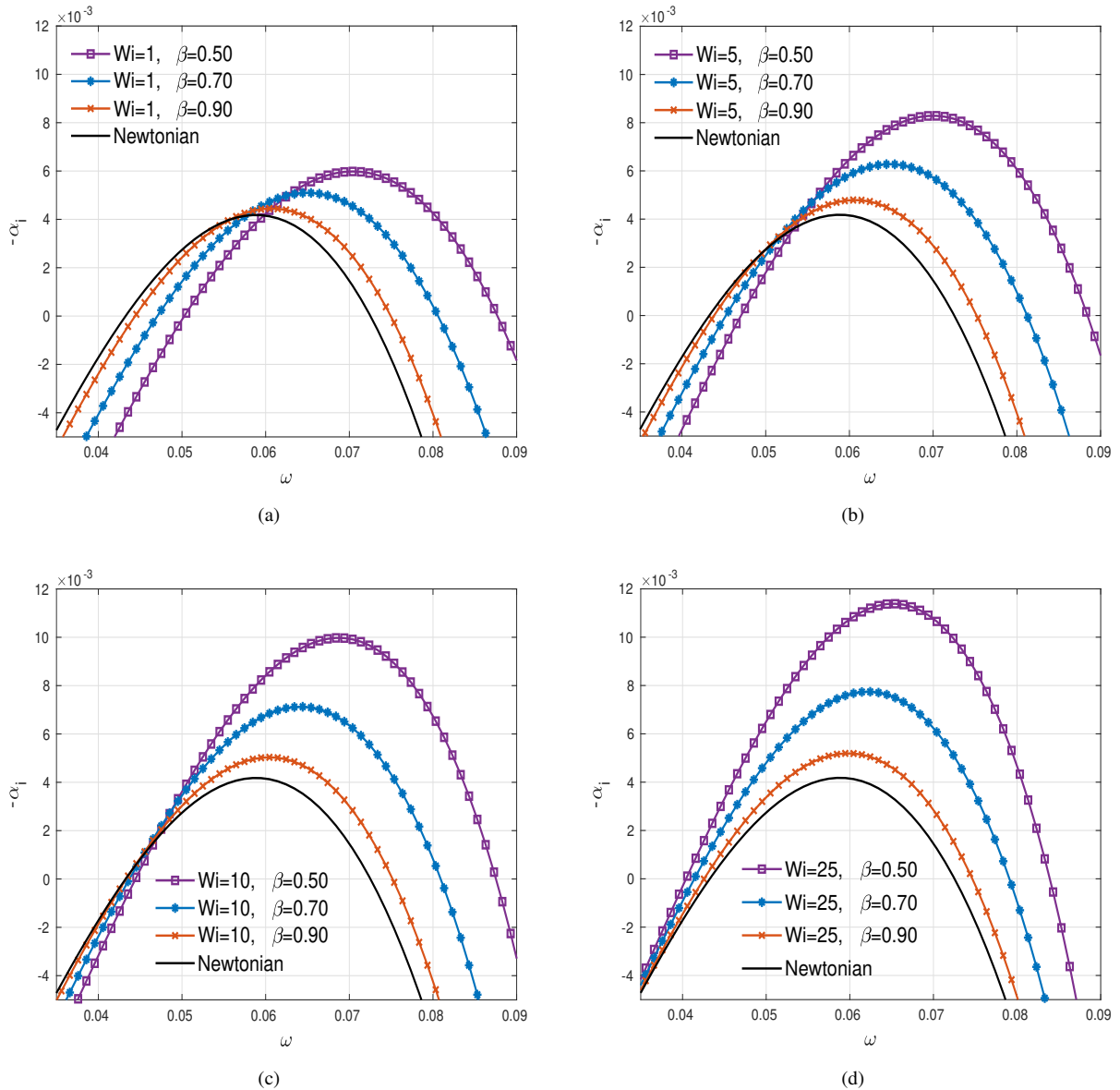


Figure 3. Amplification rate of disturbances considering β variations with: (a) $Wi = 1$; (b) $Wi = 5$; (c) $Wi = 10$ and (d) $Wi = 5$.

5. CONCLUSIONS

In this work, the Linear Stability Theory was used to investigate the hydrodynamic stability in a boundary layer flow over a flat plate, considering a viscoelastic fluid of the Giesekus type. In order to evaluate the spatial amplification rates of the disturbances, different simulations were performed, varying the dimensionless parameters that characterized the non-Newtonian fluid flow and compared with Newtonian fluid results.

The results obtained allow us to verify that non-Newtonian fluids flows are more unstable than Newtonian fluid flows since the variation of the constant β , which is directly related to the non-Newtonian contribution in the fluid, interfered in the range of unstable frequencies of the flows, and flows with lower values of β reach the highest amplification rates.

Through the Weissenberg number variation, it was also possible to analyze the effect of elastic forces on the flow stability, in the sense that the increases in Wi were able to significantly influence the flow stability, especially in fluids with a higher polymeric contribution.

6. ACKNOWLEDGEMENTS

The authors acknowledge the National Council for Scientific and Technological Development (CNPq) or the research grant received during the development of this study. The research was carried out using the computational resource of the Center for Mathematical Applied to Industry (CeMEAI), funded by FAPESP (Process Number 2013/07375-0).

7. REFERENCES

- Amoo, L.M. and Fagbenle, R.L., 2020. “Overview of non-newtonian boundary layer flows and heat transfer”. In *Applications of Heat, Mass and Fluid Boundary Layers*, Woodhead Publishing, Woodhead Publishing Series in Energy, pp. 413–435.
- Brandi, A.C., Mendonça, M.T. and de Souza, L.F., 2017. “Comparação de DNS e LST para o escoamento de Poiseuille do fluido Oldroyd-B”. In *13º Congresso Ibero-americano de Engenharia Mecânica*. Lisboa, Portugal.
- Brandi, A.C., Mendonça, M.T. and Souza, L.F., 2019. “DNS and LST stability analysis of Oldroyd-B fluid in a flow between two parallel plates”. *Journal Non-Newtonian Fluid Mechanics*, Vol. 267, pp. 14–27.
- Don, W.S. and Solomonoff, A., 1995. “Accuracy and speed in computing the chebyshev collocation derivative”. *SIAM Journal on Scientific Computing*, Vol. 16, No. 6, p. 1253–1268.
- Furlan, L., 2018. *Análise de Estabilidade de Escoamentos do Fluido Viscoelástico Giesekus*. Master’s thesis, FCT-UNESP, Presidente Prudente.
- Gervazoni, E., 2016. *Análise de estabilidade linear de escoamentos bidimensionais do fluido Oldroyd-B*. Master’s thesis, FCT-UNESP, Presidente Prudente.
- Giesekus, H., 1982. “A simple constitutive equation for polymer fluids based on the concept of deformation-dependent tensorial mobility”. *Journal of Non-Newtonian Fluid Mechanics*, Vol. 11, pp. 69–109.
- Schlichting, H., 1979. *Boundary-Layer Theory*. McGraw-Hill, IncH.
- Souza, L.F., Mendonça, M.T. and Medeiros, M.A.F., 2005. “The advantages of using highorder finite differences schemes in laminar-turbulent transition studies”. *International Journal for Numerical Methods Fluids*, Vol. 48, pp. 565–592.
- Zhang, M., Lashgari, I., Zaki, T.A. and Brandt, L., 2013. “Linear stability analysis of channel flow of viscoelastic oldroyd-B and FENE-P fluids”. *Journal of Fluid Mechanics*, Vol. 737, p. 249–279.

8. RESPONSIBILITY NOTICE

The authors are the only ones responsible for the printed material included in this paper.